
Proceedings Paper:
Irshad, A, Andrews, GE, Phylaktou, HN et al. (5 more authors) (2014) Use of the Cone Calorimeter for investigating biomass gasification combustion. In: 22nd European Biomass Conference and Exhibition Setting the course for a biobased economy. 22nd European Biomass Conference and Exhibition Setting the course for a biobased economy, 23-26 Jun 2014, Hamburg, Germany. .

Presented at the 22nd European biomass Conference & Exhibition 22nd - 26th June 2014

USE OF CONE CALORIMETER FOR INVESTIGATING BIOMASS GASIFICATION STAGED COMBUSTION

Irshad, A., Alarifi, A., Thompson, S., Melton, C.J., Andrews, G.E., Gibbs, B.M. and Phylaktou, H.N.
Energy Research Institute, School of Chemical and Process Engineering, University of Leeds, Leeds, LS2 9JT, UK.

ABSTRACT: A modified, bench scale cone calorimeter was used, at 50 and 70 kW/m^2 radiant flux, for the investigation of the gasification stage of two stage combustion of solid biomass. Pine and ash samples were investigated. The test material was supported on a load cell and contained in an air tight box, where the air flow was controlled to give an overall rich atmosphere equivalent to 1st stage gasification conditions. The gasification products flowed through the truncated top of the conical heater into a discharge duct where they were continually sampled through a heated line into a heated Temet Gasmet FTIR analyser. Secondary air was entrained after discharge from the duct, representing the lean second stage combustion in two stage biomass combustion. The total mixed product flow was used to determine the total overall heat release rate by oxygen consumption calorimetry. The primary zone showed flaming and char burning phases. Rich gasification equivalence ratios were generated depending on the fuel type and the gasification zone air supply. The optimum gasification stage conditions could be determined for maximum CO and hydrogen. The cone calorimeter was shown as a viable analytical method for determining the optimum 1st stage gasification conditions for different biomass fuels.
Keywords: cone calorimeter, load cell, gasification, heat release rate, oxygen consumption calorimetry

1 INTRODUCTION

Biomass, especially wood, is an alternative to fossil fuels for CO_2 reduction [1]. All solid biomass combustion systems, whether pellet, chip or log fired, use two stage burning where the combustion air is split into two with only the first stream passing to a fuel chamber [2-5]. The initial combustion occurs rich and undergoes gasification reactions to generate CO and H_2 and then secondary air is added. However, in most staged combustion designs that primary and seconday air split is fixed by the ratio of two flow divider areas. Biomass has a wide range of HCO composition and the stoichiometric air to fuel ratio (A/F) by mass can vary between 4 and 8, depending on the biomass source. If it was desired to optimise the flow split so that each biomass had optimum gasification conditions then optimisation of the air flow split as well as the total air flow with biomass A/F would be dependent on the biomass.

The major use of gasification, particularly for biomass, is in the thermal heat or small scale steam turbine power plants up to around 50MW [2]. There is also a high potential for use of solid biomass boilers for small-scale space and water heating. Biomass gasification boilers operate at comparable thermal efficiencies to that of fossil fuel types In constrast large scale biomass power for electricity uses pulverised biomass premixed with air, often co-fired with coal. The mechamism of burner of fine (~ 50 - 500µm) biomass powders surrounded by surplus air is quite different from logs and chips, where the heat transfer through the thickness of the material is an important part of the combustion process.

This work was carried out to show a practical small scale test that could be used for the characterisation of solid biomass used with air staging, so that there was a gasification first stage rich burning zone that could be optimised for each biomass. The method uses the cone calorimeter equipment which has proved successful in the study of material behaviour in fires.

The cone calorimeter is a common instrument in fire research, where it is used to characterise the ignition heat flux of materials, to determine the heat release rate and to assess the effectiveness of fire protection methods such as material coatings or fire retardant performance. Considering that one of the most common fire materials is wood (as about 50% of all fires involve wood as the main fuel), then the relevance to biomass combustion is obvious.

The cone calorimeter uses a conical electrical heater to heat the test specimen and is calibrated to be able to achieve 10 – 70 kW/m^2 uniform heating of the test surface. This can be varied to determine the incident heat flux that will ignite materials. The radiant heat represents the behaviour of the material in a fire surrounded by other flames and hot surfaces that radiate to the specimen. This principle is also applicable to more general biomass combustion using relatively small samples that are burning in a similar way that they would in a much larger combustor biomass burning zone. A modification to the cone calorimeter enables a sealed box with a glass window to surround the test specimen. This allows the atmosphere around the test material to be controlled [6] and in the present work this was used to meter the combustion air supply to the wood specimen so that combustion occurred under rich conditions with the major products being CO and H_2, which is gasification.

Much of the literature on gasification has been directed at gas turbine applications where a separate gasifier is used to generate the CO & H_2 gas, often with steam added to enhance the H_2 yield through the water gas shift reaction. This gasification gas is then burned with air in a gas turbine combustor. Much of the work in this area is based on pure oxygen gasifiers to keep nitrogen out of the gas and to improve the calorific value. However, there are very few of these plants operational around the world using fossil fuels and none large scale for biomass. In contrast there are many biomass gasification heaters and small scale boilers which use air as the gasifier oxidant. These biomass heaters link the heat release from the gasifying zone directly to the secondary zone as the ideal systems would operate the gasifying zone adiabatically and then extract all the heat in the secondary zone after completion of second stage combustion. It is this type of staged gasification biomass heaters that the present work is directed at.

2 MATERIALS AND METHODS

2.1 Biomass characterization

Samples of ash wood and pine wood in the physical arrangement described below, were used in the present

work. A Thermo Flash EA 2000 was used for the ultimate elemental analysis of the wood samples. A TGA-50 Shimadzu TGA with a TA60WS processor was used for the proximate analysis of water, volatiles, fixed carbon and ash content of the wood. A Parr 6200 oxygen bomb calorimeter was utilized for determination of the gross calorific value of the biomass samples. The analytical results are shown in Table I.

Table I: Ultimate and proximate analysis of biomass samples

Parameter	Pine wood	Ash wood
Proximate analysis (wt.%) (daf)		
Volatile matter	86.35	90.44
Fixed carbon	13.65	9.56
Ultimate analysis (wt.%)(daf)		
Carbon	51.55	50.30
Hydrogen	6.13	6.14
Nitrogen	0.54	1.09
Sulfur	0.00	0.00
Oxygen	41.77	42.47
GCV (MJ/kg)	19.2	18.26
Moisture (as received)	6.54	4.13
Ash (as received)	2.00	7.60

2.2 The cone calorimeter

For the present work, a cone calorimeter was used with the 'fire atmosphere' sealed enclosure box around the test specimen, as shown in Fig. 1. This was a 38 cm long, 30 cm wide and 33 cm high air sealed box. This box was supplied with a metered air flow so that the global equivalence ratio, ϕ, of the combustion or gasification could be controlled.

The biomasses used in the present work were sticks of pine and round ash wood (sometimes referred to as 'brash') of nominal diameter/square-side of 20mm and 100mm long, and were placed in the 100mm square test section of the cone calorimeter. Only the top surface of the specimen was exposed to the radiation and air. For the pine samples this was a flat surface, but for the ash / brash it was five hemispherical surfaces, with ash bark exposed to the radiation.

A metered flow of primary air was supplied to this sealed box from two openings in the bottom. A calibrated variable area flow meter was used to determine the air flow. The air flow has been expressed in the results as flow per 100 mm square surface area of the test specimen, g/(m^2.s). This was to enable the results to be scaled to other dimensions of gasification bed size.

The biomass fuel load in the 100mm square test holder was mounted on a load cell so that the A/F by mass could be determined as a function of time during the test. This load cell should be water cooled as it lies inside the fire box, this was missing in the present work an limited the heat flux used to well below the 100 kW/m^2 of the base test equipment. However, 50 kW/m^2 is a high enough radiant flux to simulate a surrounding biomass flame in a larger burner [7].

The test conditions in terms of air flow rate, biomass and radiant flux are summarized in Table II. In some of the tests thermocouples were inserted into the biomass near the top surface and near the bottom surface. These were used to determine the time of the thermal conduction of the radiant heat and flame heat inside the specimen, which controlled the thermal gasification zone as it passed through the thickness of the biomass.

The insertion of thermocouples affected the operation of the load cell and these tests were carried out as separate tests and were not done at the same time as the mass loss measurements. One thermocouple was inserted from the side through the wall of the air enclosure 5 mm from the top surface of the sqaure pine wood and the other was placed 35 mm from the top of the sample (5 mm from the bottom). This was done in the tests in Table II where two pine wood stick heights were used to give the total thickness of the sample as 40 mm. For the other tests in Table II the sample thickness was 20mm.

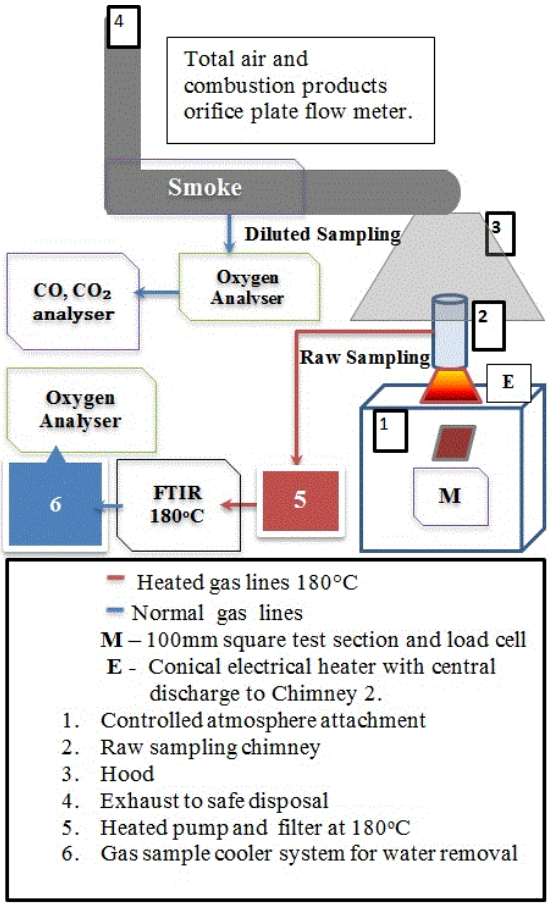

Figure 1: Cone calorimeter equipment schematic

Table II: Conditions for the tests performed

Biomass	Quantity No. of sticks	Inlet air flow rate g/(m^2.s)	Heat flux kW/m^2
Pine wood	5	9.0	70
Pine wood	5	9.8	70
Ash wood	5	9.0	70
Pine wood	5	12.8	50
Pine wood	5	19.2	50
Pine wood	5	25.6	50
Pine wood	10	12.8	70
Pine wood	10	14.0	50

This enclosure box had a glass window for observation of the biomass flame throughout the test. The biomass sample was exposed to the conical heater of the cone calorimeter that was radiating 50 – 70 kW/m^2 of heat flux depending on the test. A chimney 21 cm high

and 8 cm in diameter was mounted on the top of the cone calorimeter heater to represent the connecting duct between the two combustion zones in biomass gasification heaters.

2.3 Gas Composition Analysis

There was a gas sample point taken using a single hole gas sampler on the centerline of the exit duct from the gasification zone (chimney) for the analysis of the gas composition from from this zone. This was connected via a stainless steel 190^{o}C heated sample line to a heated sample pump and filter and then via a further heated sample line to a heated Temet GASMET CR-series FTIR spectrometer. This was a purpose built portable FTIR that has UK Environmental Agency MCERT approval for legislated flue gas composition measurements. It was calibrated by the manufacturers for 60 gaseous species and has been used for in-vehicle real world exhaust gas measurements as well as for fire toxicity work using the present equipment as well as in larger scale compartment fires. This analyser uses a liquid nitrogen cooled photo-detector that gives it ppm resolution of most gases. As it is fully heated it measures the total water vapour present in the sample and this feature was used in the present work to follow the water release from biomass as it was heated. The full range of combustion generated gases including CO, CO_2, NO, NO_2, HCN, NH_3, N_2O, CH_4 and a range of other hydrocarbons and aldehydes. The objective of the present work is to concentrate on the main species of H_2O, CO_2 and CO. Hydrogen is not absorbed by infra red and cannot be detected by an FTIR; It was calculated from the water gas shift reaction, as in equilibrium with the CO measurements.

Downstream of the FTIR gas outlet there was a sample water cooler and silica gel column to remove the water vapour from the gas sample. This dry gas sample was then fed to a paramagnetic oxygen analyzer for the measurement of oxygen in the gas sample from the chimney (raw gas sample) and for the determination of the heat release rate (HRR) of the gasification zone by oxygen consumption calorimetry. The water vapour measured by the FTIR was then used to correct the oxygen reading from a dry to a wet gas basis prior to the oxygen consumption calorimetry calculations, as discussed below.

Secondary combustion was not the main aim of the present work, but the gases from the exit of the chimney from the gasification zone were mixed with the secondary entrained air and flowed to the cone calorimetry standard measurement system. The air dilution gave rise to oxidation of the CO and hydrogen from the gasification zone, but this was not the most efficient process as there was no forced mixing of the air and gasified gases. In future work the addition of a mixing burner at this point will be investigated.

The total flow through the exhaust duct, into which the discharge from the gasification zone was directed, was set at 24 l/s for all tests. This exhaust duct contained another sampling point for oxygen measurement and hence the calculation of the total heat release rate of both combustion stages. There was an extract fan downstream in the exhaust duct and an orifice plate for total flow measurement using the differential pressure across the orifice. The oxygen measured in this diluted sample was used to compute the total primary and secondary HRR. In addition the total overall HRR was determined from the mass loss rate times the biomass calorific value. If combustion was complete in the secondary air mixing zone then these two HRR should be the same. However, if there is a difference then this indicates that the mixing in the secondary zone was inadequate to burn the CO and H_2 from the gasification zone.

2.4 Equivalence ratio (ϕ)

The equivalence ratio is the ratio of the stoichiometric air to fuel ratio $(A/F)_S$ to that of measured air to fuel ratio by mass $(A/F)_M$ [8]. ϕ >1 denotes a rich mixture where the air is insufficient to burn all the fuel. and yields increasing CO and H_2 as ϕ increases. ϕ = 1 indicates a stochiometric mixture and ϕ < 1 indicates a lean mixture, which is the overall condition of the diluted sample in the cone calorimeter duct. The inflluence of overall excess air was not the purpose of the present work. The stoichiometric A/F was determined in Table I and is shown in Table III on a dry ash free (daf) basis and an actual composition basis (including the water and ash in the biomass composition). The equivalence ratio denoted as ϕ_{total} was calculated based on the actual solid fuel composition basis stoichiometric A/F.Table III shows that the two woods were very similar with only 6 % difference in their stoichiometric A/F by mass. Table I shows that the biggest difference was in the higher ash content of ash-wood.

Table III: Stoichiometric air to fuel ratio for biomass

Biomass	y = H/C daf	z = O/C daf	Elemental formula CH_yO_z	$(A/F)_S$ daf	$(A/F)_S$ Actual basis
Pine wood	1.43	0.61	$CH_{1.43}O_{0.61}$	6.27	5.74
Ash wood	1.46	0.63	$CH_{1.46}O_{0.63}$	6.13	5.42

2.5 Heat release rate (HRR) calculations

The HRR was calculated by two methods, one based on the biomass mass loss rate (MLR) and the other based on the principle of oxygen consumption calorimetry which requires the air mass flow rate and the oxygen concentration downstream of the combustion zone. The relationship between HRR and MLR is given by equation.

$$HRR = \Delta h_c \times MLR \quad (1)$$

where

Δh_c = net heat of combustion (kJ/g)

Oxygen consumption calorimetry is based on the fact that a constant amount of heat is released per kg of oxygen consumed, for complete combustion of liquid or solid fuels. Hugget [9] found the value of this constant to be 13.1 kJ/g of oxygen with an accuracy of ± 5 % or better . The generalized HRR is given in equations below [10].

$$\dot{q} = E.\left(\dot{m}_a Y_{O_2}^a - \dot{m}_e Y_{O_2}^e \right) \quad (2)$$

Where

$\dot{q}$	heat release rate kW
E	net heat released per unit mass of oxygen consumed 13.1 kJ/g of oxygen
$\dot{m}_a$	mass flow rate of inlet (ambient) air
$\dot{m}_e$	mass flow rate of exhaust

$Y_{O_2}^{a}$ mass fraction of oxygen in ambient air (0.232 g/g air)

$Y_{O_2}^{e}$ mass fraction of oxygen in combustion products

As discussed above, there were two oxygen sampling points, one after primary gasification zone (enclosed box) and other in the exhaust duct to measure corresponding heat release rates by oxygen consumption calorimetry.

2.6 Carbon monoxide emission index (EI_{CO})

The Emission Index (EI) is defined as [11]

$$EI = \frac{\text{mass emsission}}{\text{mass of fuel}}$$

The EI is related to the volumetric species concentraion C and the exhaust A/F by mass

$$\text{Or } EI = K \times C \times \left[1 + \left(\frac{A}{F}\right)\right] \times 1000 \text{ g/kg fuel} \qquad (3)$$

where

K = Ratio of molecular weight of the gas component to that of the exhaust sample.

For many combustion situations the molecular weight of the exhaust gases is approximately equal to that of air to less than 2% error. For CO the K value is 0.968 if the concentration C is a fraction, with appropriate conversion used if tis actual measurement is % or ppm. The combustion inefficiency due to CO, hydrogen and hydrocarbons can be determined from Eq. 3 by multiplying by the CV kJ/g for each component and dividing by the CV of the biomass. This is then an energy ratio which is the % of the original biomass energy that remains in the CO, H_2 and hydrocarbons that flow from the gasification zone into the secondary combustion zone.

3. EQUILIBRIUM CALCULATIONS

Adiabatic equilibrium models can be used to estimate the maximum achievable equilibrium yields of CO, H_2 and other gases during adiabatic rich combustion which is essentially gasification. The input is the elemental composition on a daf basis and the gross calorific value of biomass, the output is the equilibrium adiabatic flame temperature and the equilibrium gas composition. The Leeds University, Energy Research Institute FLAME computer programme was used in this study. FLAME calculates the mole fractions of gasification products as a function of excess air factor lambda (λ) which is the reciprocal of the equivalence ratio (ϕ). λ is the ratio of real air requirements of a fuel to the theoretical air requiremnt of the fuel [12].

Equilibrium calculations for dry ash and pine wood were performed using the values of excess air factor from 0.1 to 1.5 and are shown in Figs. 2 and 3 for ash and pine woods respectively.

The calculations show that for ash wood the maximum combined volume concentration of CO and H_2 was predicted to be 44% and values of λ where CO + H_2 were > 40% spanned 0.16 to 0.36 (ϕ 6.25 to 2.7). For pine wood the corresponding values of λ range from 0.2 to 0.36. (ϕ from 5 to 2.7).

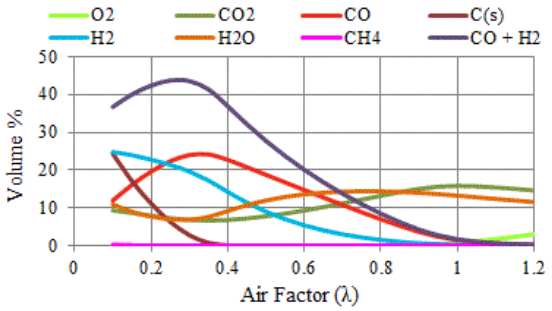

Figure 2: Equilibrium concentrations of gaseous products as a function of air factor (λ) for ash wood gasification

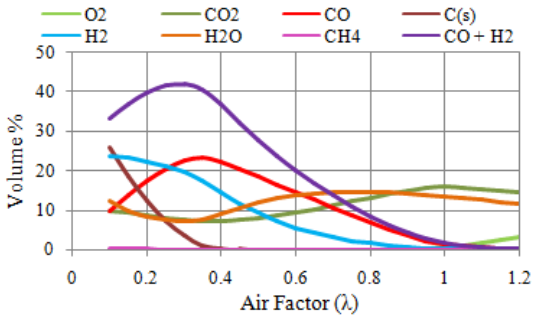

Figure 3: Equilibrium concentrations of gaseous products as a function of air factor (λ) for pine wood gasification

For the cone calorimeter experimental conditions to come close to these equilibrium predictions the rich combustion or gasification zone should be adiabatic and as close to the rich mixture adiabatic temperature as possible. The problem with the present use of the cone calorimeter (to investigate the rich gasification burning) was that these conditions were not met and the burning zone was at too low a temperature. The results show that very inefficient gasification resulted.

This means that in a practical gasification air staged heater, the gasification zone should be insulated so that it operates at the highest temperature close to the equilibrium temperature. Also the gasification zone should have sufficient residence time to reach equilibrium. Both of these conditions should ensure that the gases passing to the second stage combustion zone should be as close to the adiabatic temperature as possible and with the highest CO and H_2 content. Any deviation from these ideal conditions will result in gasification and combustion inefficiencies. If hydrocarbons, oxygen or water vapour are present in the gasification zone outlet then this is non-ideal or inefficient gasification. If the zone outlet temperature is below the adiabatic then there is a thermal efficiency loss.

In practice most gasification staged biomass heaters do not come close to these ideal conditions. Many deliberately water cool the gasification zone,, which ensures that thermal losses do not occur, but also ensures inefficient gasification as the zone temperature will be too low. It would be preferably to externally air cool the gasification zone prior to the air feeding the gasification zone. This would ensure that any heat passing through

the gasifier ceramic walls would be recovered and recycled back into the zone. The present small scale gasification zone was far from adiabatic as the air cooled chamber was not insulated, this was because of the problem of overheating the load cell. This will be solved in future work by water cooling the load cell. It will also be shown that CO concentrations were below those expected from adiabatic gasification.

4 RESULTS AND DISCUSSION

4.1 Mass loss of samples

The biomass sample mass and rate of mass loss as a function of time during gasification are shown in Figs.4 and 5 respectively, for all tests in Table II with five wood sticks in the 100mm square test section. Figs. 4 and 5 show that there were two stages to the gasification: an initial relatively high mass loss rate followed by a slower mass loss rate at the end of the wood burn out. The transition between these two stages was observed to coincide with the transition between flaming combustion and char combustion. This is most clearly seen for the ash sample with 70 kW/m^2 heating. Pine wood at the same conditions clearly gasified at a slower rate. This could be due to the outer bark on the ash sample and the effectively greater surface area from the five round brash branches. Fig. 3 shows that the char burning stage for ash and pine was about 17% of the initial mass for 70 kW/m^2. For the lower heating rate of 50 kW/m^2 the flaming combustion mass loss rate for pine was lower and for three air flow rates was between 0.05 and 0.06 g/s compared with 0.07-0.08 g/s for pine at 70 kW/m^2.

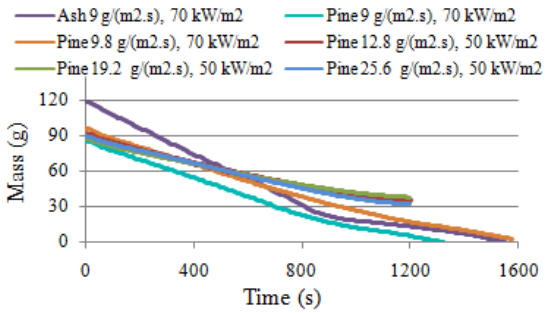

Figure 4: Mass vs time for tests with 5 wood sticks

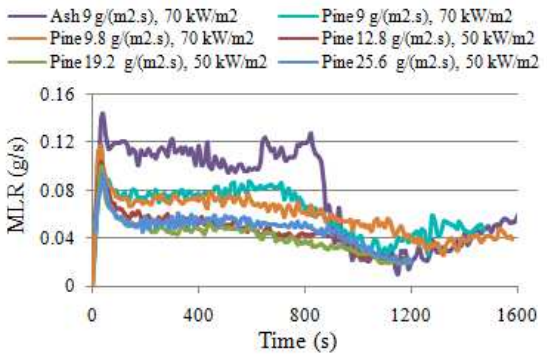

Figure 5: Mass loss rate for 5 wood sticks.

The char burn out stage represents inefficient gasification. It is shown below that there is little production of CO. The reason is that the air flow to the gasification zone is constant and so as the mass burning rate slows in the char phase, the equivalence ratio of the zone moves towards stoichiometric. The result is that most of the char burns to CO_2 which is undesirable. In a practical gasification burner this would not be an operational condition as more biomass would be added as to the gasification zone. Thus, in the present work this second stage char burnout will be ignored as gasifiers are not normally operated to allow total burn-out.

In the test with a heat flux of 70 kW/m^2, ignition for pine wood started after 6 s and for ash wood it started after 13 s. In the tests of 5 pine wood sticks with 50 kW/m^2 heat flux, ignition started in 8, 11 and 16 s for air flow rates of 12.8, 19.2 and 25.6 g/(m^2.s) respectively. This first stage, in which vigorous drying and devolatilisation of sample takes place, lasts for 40-70 seconds, as can be seen in Fig 5.

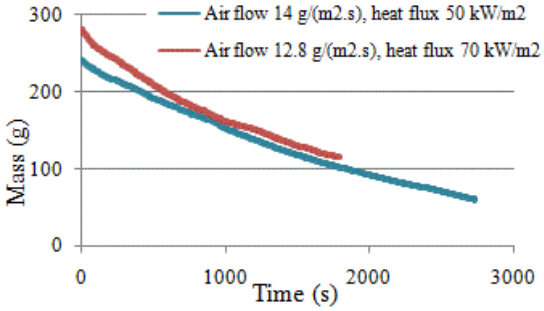

Figure 6: Mass vs time for tests with 10 pine wood sticks (2 layers)

For tests with 10 pine wood sticks (in two layers) and air flow of 12.8 g/(m^2.s) at 70 kW/m^2 and 14 g/(m^2.s) at 50 kW/m^2 a similar mass loss trend was found to that with the thinner pine wood load, as shown in Figs. 6 and 7. However, there was a significant difference in that the rate of burning decreased with time, rather than the constant rate in the flaming combustion stage for the single layer test. The initial flaming combustion mass loss rate decreased from 0.11 to 0.05 g/s over the 1800s flaming combustion phase, compared with 0.06 g/s for the thinner sample.

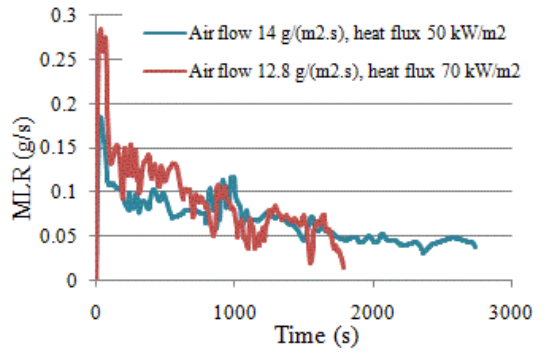

Figure 7: Mass loss rate for tests with 10 pine wood sticks (2 layers)

The faster initial burn rate for the thicker sample was possibly a result of the thicker pine wood acting as a self insulation so that the surface temperature exposed to the

radiation was hotter. Also the release of volatiles from the flaming zone propagating through the thickness would result in the initial char layer burning in the products of gas release from deeper within the wood. The results for the thicker specimen were not continued to completion of the char burn out, as this phase was not of major interest. Essentially in this work once the thicker wood had burned down to the same mass as the thinner layer started with, the mass burn rates were similar. As for the thinner layer, an increase in radiation from 50 to 70 kW/m^2 led to an increase in the mass burn rate.

4.2 Measured ϕ_{total}

The measured A/F for the thin and thick wood samples were determined and converted to an equivalence ratio, ϕ_{total}, which is shown as a function of time in Figs. 8 and 9. The higher mass loss rates lead to richer mixtures as the air flow is constant. Figs. 8 and 9 show that the aim of this work to create rich burning gasification conditions was achieved. The equivalence ratio could be varied by changing the air flow or the heating rate.

For comparison with the equilibrium model, values of ϕ_{total} obtained in steady state flame combustion stage were converted to λ for all tests and are shown in the table IV.

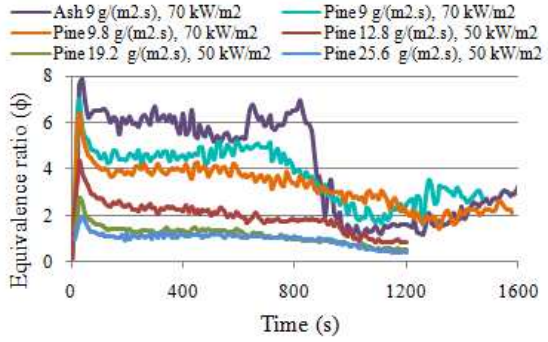

Figure 8: Equivalence ratio (ϕ_{total}) for tests with 5 wood sticks

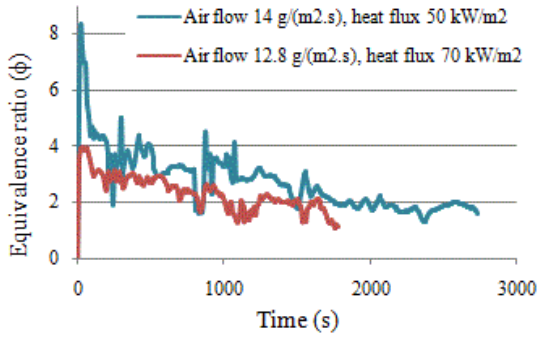

Figure 9: Equivalence ratio (ϕ_{total}) for tests with 10 pine wood sticks (2 layers)

For optimum gasification, the equilibrium model predicted the values of λ for ash wood from 0.16 to 0.36 and for pine wood from 0.2 to 0.36 (see Figs 2 and 3). Table IV shows that the tests with 5 pine wood sticks at 9 g/(m^2.s), 5 pine wood sticks at 9.8 g/(m^2.s), 10 pine wood sticks at 14 g/(m^2.s) had optimum values of λ.

4.3 Heat release rate (HRR)

The total HRR for all the tests was calculated based on the MLR as well as based on oxygen consumption calorimetry. The primary zone HRR based on oxygen consumption calorimetry was also calculated. The difference between total HRR and primary zone HRR gives secondary zone HRR. Primary and secondary HRR were evaluated as percentages (%) of the total HRR as shown in Figs. 10-16.

Table IV: Equilibrium CO and H2 concentrations against measured air factor (λ) in the steady state flame combustion stage

Sample	Air flow rate and heat flux	λ (flame combustion stage)	Eq. CO Vol. %	Eq.H_2 Vol. %
5 ash sticks	9 g/(m^2.s), 70 kW/m^2	0.15	16	24
5 pine sticks	9 g/(m^2.s), 70 kW/m^2	0.20	17.5	22.5
5 pine sticks	9.8 g/(m^2.s), 70 kW/m^2	0.24	20.0	21.5
5 pine sticks	12.8 g/(m^2.s), 50 kW/m^2	0.45	20.5	11.5
5 pine sticks	19.2 g/(m^2.s), 50 kW/m^2	0.71	10.0	1.5
5 pine sticks	25.6 g/(m^2.s), 50 kW/m^2	0.83	6.0	1.0
10 pine sticks	12.8 g/(m^2.s), 70 kW/m^2	0.40	22.0	14.0
10 pine sticks	14 g/(m^2.s), 50 kW/m^2	0.30	22.0	19.0

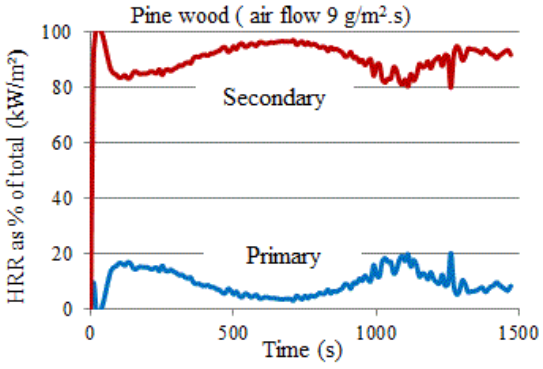

Figure 10: Primary and secondary HRR expressed as % of total, for pine wood at air flow 9 g/(m^2.s) and heat flux 70 kW/m^2

In the tests of 10 pine wood sticks the primary HRR in the steady state flame combustion zone was 10% for the test with air flow 12.8 g/(m^2.s) and heat flux 70 kW/m^2 and 20% for test with air flow 14 g/(m^2.s) and heat flux 50 kW/m^2, showing that primary gasification zone successfully acted as a gasifier in the flame combustion zone for the test conditions.

For the thinner 20mm thick wood load there were conditions where ideal gasification HRR conditions were achieved with the proportion of HRR in the gasification zone being low. These are summarized in Table V, which

shows that the 70 kW/m^2 radiation flux, which would control the biomass gasification temperature, was necessary to get rich flaming combustion at < 20% of the heat release for the ash and pine biomass. Both woods had very rich gasification zone ϕ_{total} of 5 – 6.8. Also this heating rate needed to be combined with a low air flow of 9 g/(m^2.s) to achieve the desired rich mixtures. These conditions are richer than the adiabatic equilibrium predictions gave.

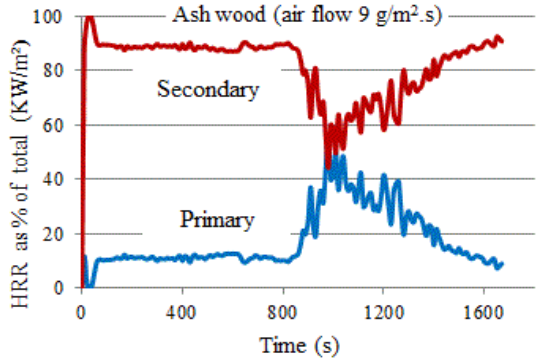

Figure 11: Primary and secondary HRR expressed as % of total, for ash wood at air flow 9 g/(m^2.s) and heat flux 70 kW/m^2

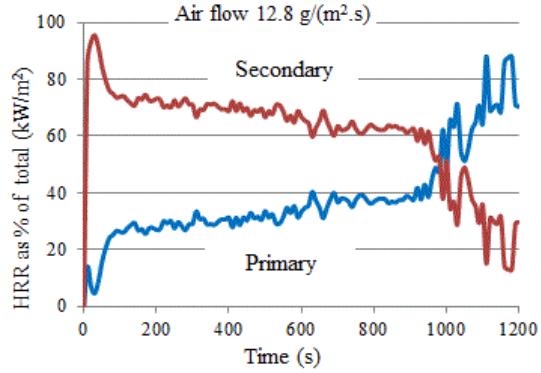

Figure 12: Primary and secondary HRR expressed as % of total, for pine wood at air flow 12.8 g/(m^2.s) and heat flux 50 kW/m^2

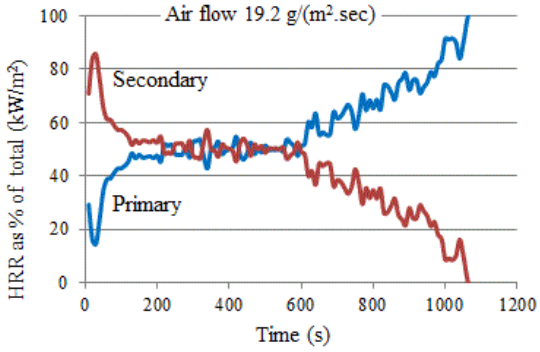

Figure 13: Primary and secondary HRR expressed as % of total, for pine wood at air flow 19.2 g/(m^2.s) and heat flux 50 kW/m^2

For the 50 kW/m^2 heating the 20mm thick pine wood increased the proportion of the HRR in the gasification stage as the air flow was increased. This increase in air flow reduced ϕ_{total} and as this reduced the proportion of HRR in the gasification zone increased until there was mainly combustion not gasification at 25.6 g/(m^2.s). For the thicker 40mm thick pine wood both test conditions gave < 25% of the HRR in the gasification zone and had ϕ_{total} ~ 3. For the thinner specimen at 50 kW/m^2 the gasification was poor and hence the sample thickness is clearly important. Normally in gasification heaters the bed thickness would be much greater than 40mm. The 70 kW/m^2 heating for the thicker sample gave good gasification at an air flow of 12.8 g/(m^2.s).

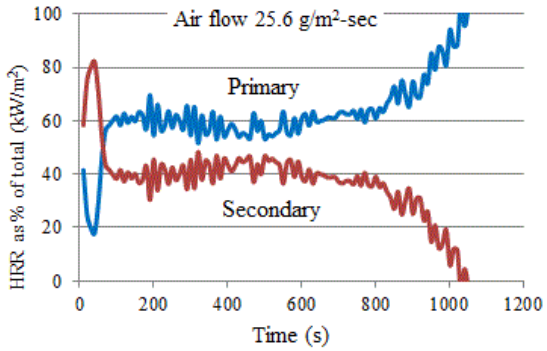

Figure 14: Primary and secondary HRR expressed as % of total, for pine wood at air flow 25.6 g/(m^2.s) and heat flux 50 kW/m^2

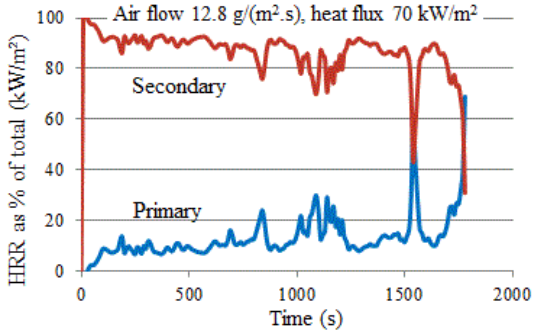

Figure 15 Primary and secondary HRR expressed as % of total, for test with 10 pine sticks (2 layers) at air flow 12.8 g/(m^2.s) and heat flux 70 kW/m^2

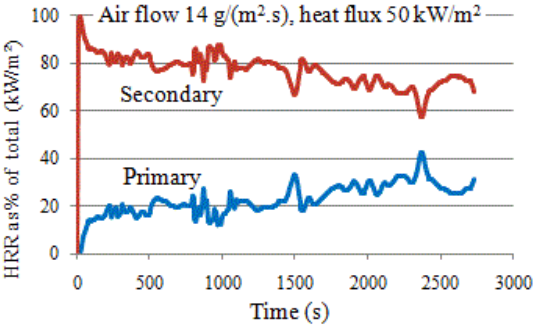

Figure 16: Primary and secondary HRR expressed as % of total, for test with 10 pine sticks (2 layers) at air flow 14 g/(m^2.s) and heat flux 50 kW/m^2

4.4 Carbon monoxide and hydrogen emissions

The percentage of CO from the raw sample from the outlet from the gasification zone is shown in Figs. 17 - 19. There was no instrument used for the measurement of H_2, so its equilibrium concentration was predicted from the measured CO using the water gas shift reaction.

$$CO_2 + H_2 \leftrightarrow CO + H_2O$$

Equilibrium constant for this reaction is given as

$$K = \frac{[CO][H_2O]}{[CO_2][H_2]}$$

where K is a function of equilibrium temperature, here a value of 3.5 is used, which corresponds to T_{eq} 1738 K [13].

Table V: Summary of test results for the main flaming rich combustion phase for the gasification zone.

Radiation kW/m^2-wood	Depth mm	Air flow g/(m^{2}s)	% HRR gasif	ϕ_{total}	CO %	CO EI g/kg
70 -ash	20	9	15	6.8	1	20
70 -pine	20	9	5 -20	5	1	20
70 -pine	20	9.8	30	4.2	1	40
50 -pine	20	12.8	30	2.2	1	20
50 -pine	20	19.2	50	1.6	1	20
50 -pine	20	25.6	60	1.2	1	20
70 -pine	40	12.8	10-20	2-3	1-3	50-100
50 -pine	40	14	20-25	3-4	1	25

It can be seen in Fig. 17 that in all tests with heat flux of 70 kW/m^2, the peak values for CO emissions were obtained during the first stage of drying and devolatilization. These values then dropped in the steady state flame combustion zone. The CO was recorded to be 13%, 10% and 3% in first stage and 3%, 1.6% and 1.5 % in the steady state flame combustion stage for pine at air flow 9.8 g/(m^2.s), pine at air flow 9 g/(m^2.s) and ash wood at air flow 9 g/(m^2.s) respectively.

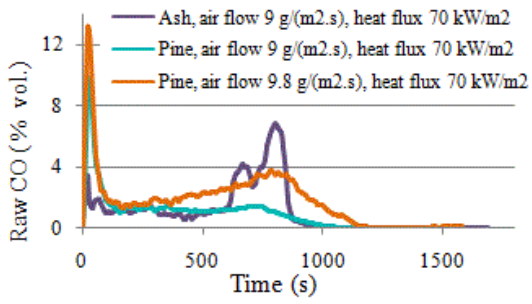

Figure 17: % CO from gasification stage for test with 5 wood sticks heat flux 70 kW/m^2

In tests with a heat flux 50 kW/m^2 (Fig. 18), the CO was 7.5, 6.5 and 4% in the first drying stage for 5 pine sticks at air flow 12.8, 19.2 and 25.6 g/(m^2.s) respectively. The CO then reduced to less than 1% and with an air flow 25.6 g/(m^2.s) in the steady state flame combustion zone.

Corresponding equilibrium % of H_2 calculated from water gas shift reaction are shown in Figs. 20 and 21.

Values of CO and H_2 were very low compared to those predicted from equilibrium model shown in Table IV. This indicates that reactions did not reach equilibrium during the test.

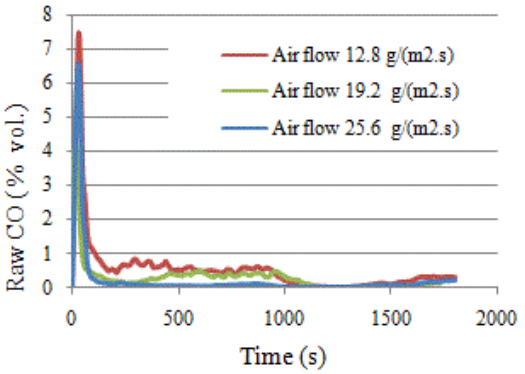

Figure 18: % CO from gasification stage for test with 5 pine wood sticks heat flux 50 kW/m^2

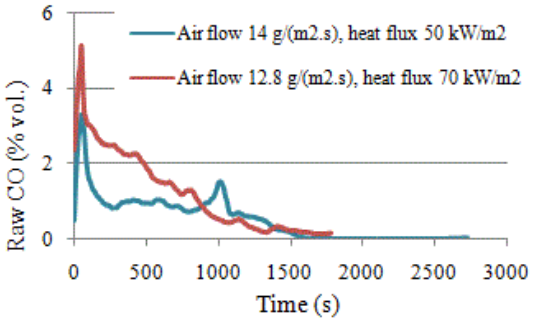

Figure 19: % CO from gasification stage for test with 10 pine wood sticks (2 layers)

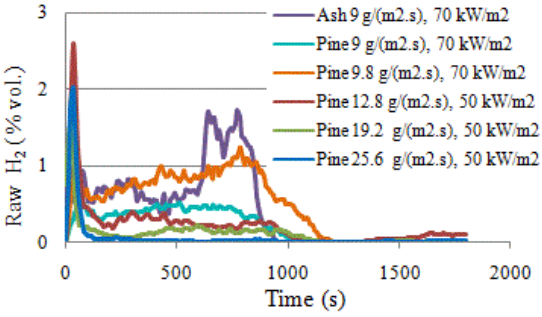

Figure 20: % H_2 from the gasification stage for test with 5 wood sticks

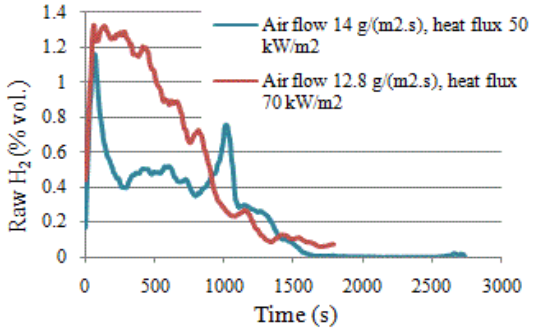

Figure 21: % H_2 from the gasification stage for test with 10 pine wood sticks (2 layers)

4.5 Carbon monoxide emission index (EI_{CO})

The EI for CO are shown in the Fig. 22 for tests with 5 wood sticks and in fig. 23 for tests with 10 pine wood sticks.

Table V compares the CO emissions during the near steady state flaming gasification stage of burning. This shows that the CO was only high (>1%) for the thick pine wood samples. This indicates that a thick bed depth is needed for gasification burning to be effective in gasification. However, the conditions of these tests are clearly well removed from equilibrium and this indicates that the heat losses in this equipment badly affect its use to study the primary stage of two stage biomass combustion.

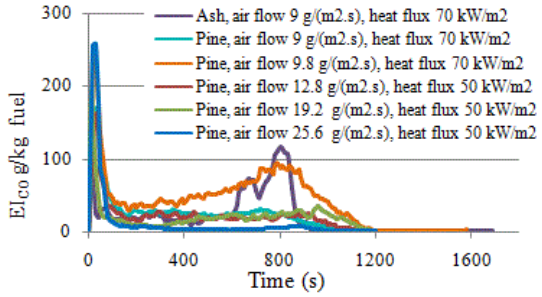

Figure 22: EI_{CO} for tests with 5 wood sticks

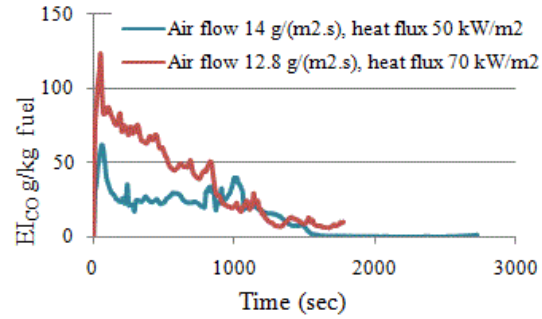

Figure 23: EI_{CO} for tests with 10 pine wood sticks

A feature of inefficient gasification due to low zone temperatures is that there will be hydrocarbons at a significant level not gasified into CO and H_2. This is shown as an example for the present results in Fig. 24. This shows that even at the highest radiant heating in the present work, which will give the highest temperature in the specimen, the total hydrocarbons (THC) were very high. This does not matter from an energy point of view as these hydrocarbons in a staged system would burn in the second stage. However, they are undesirable as they are the source of soot emissions from biomass combustion.

4.6 Temperature rise of the pine wood

Temperature rise for the tests with 10 pine wood sticks and a 40mm depth are shown in Fig. 25 at an inlet air flow of 12.8 (g/m^2.s) and in Fig. 26 for an air flow of 14 g/(m^2.s). This shows the way the thermal wave travels through the wood samples and that adiabatic saturation temperature was not achieved.

In the future insulation of the gasification zone will be used to increase the zone temperature. The present results show that 70 kW/m^2 radiant flux was required for the best gasification and this would be partially because the zone was hotter. Also low air flow rates of about 10 g/(m^2.s) gave the best results. The other significant factor was that thicker wood depths of at least 40mm gave the best gasification.

A feature of the slow thermal heating of the wood is that there is a continual relase of water vapour during the gasification stage and the water is not flashed off as it is in pulverised biomass combustion. This is illustrated as an example in Fig. 27. Water vapour is realease for up to 1000s in the experiments and Figs. 25 and 26 show that this is about the time it takes for the thermal wave to propagate through the thickness of the specimen. Whether any of this water vapour which passes through the gasification zone undergoes the water gas shift reaction with CO to produce addition hydrogen will be the subject of future work.

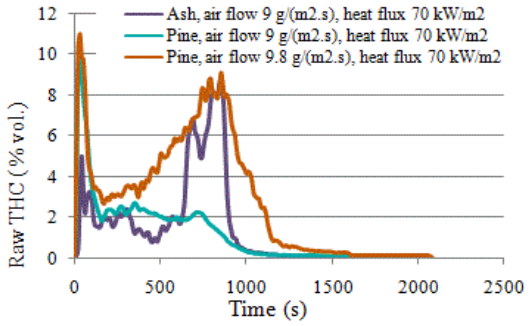

Figure 24: THC emissions during gasification of 5 wood sticks at heat flux 70 kW/m^2

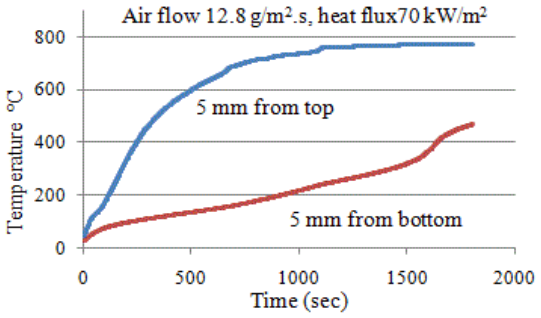

Figure 25: Temperature vs time for test with 10 pine wood sticks (2 layers) inlet air flow 12.8 g/(m^2.s), heat flux 70 kW/m^2

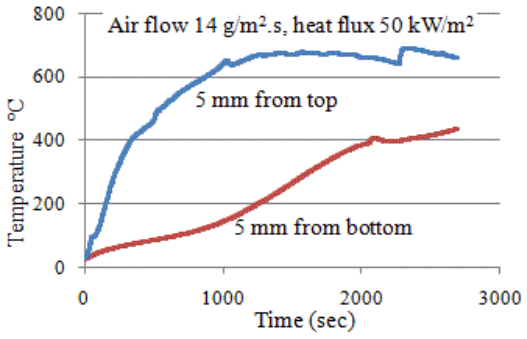

Figure 26: Temperature vs time for test with 10 pine wood sticks (2 layers) inlet air flow 14 g/(m^2.s), heat flux 50 kW/m^2

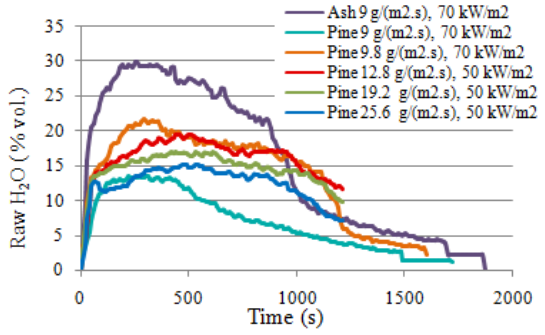

Figure 27: Water vapour released during rich combustion heating of 'dry' biomass.

6 CONCLUSIONS

A modified, bench scale cone calorimeter was used to investigate the gasification stage of a log-gasification boiler using pine and ash wood samples. It was shown that this experimental technique could give useful information on staged biomass combustion and is recommended as an additional laboratory test in the evaluation of biomass fuel properties.

The equivalence ratio (ϕ_{total}) in the steady state flame combustion zone acquired an average values of 6.8, 5 and 4.2, for 5 sticks of ash wood, pine with air flow 9 g/(m^2.s) and pine wood with air flow 9.8 g/(m^2.s) at 70 kW/m^2 respectively. Also in tests of 10 pine wood sticks at air flow 14 g/(m^2.s) at heat flux 50 kW/m^2 and 12.8 g/(m^2.s) at 70 kW/m^2 equivalence ratio was 3 and 2.5 respectively in steady state flame combustion zone. All these conditions are rich burning showing that the enclosure box of the cone calorimeter attained gasification conditions. At flow rates of 12.8, 19.2 and 25.6 g/(m^2.s) the equivalence ratio in steady state flame combustion was 2.2, 1.4 and 1.2 respectively at 50 kW/m^2 with 5 pine wood sticks showing that combustion conditions were only slighly at high air flow rates and good gasification was not achieved.

These equivalence ratios, when compared with the prediction of the FLAME equilibrium model, indicated that the fuel-air mixture in this study was too rich for some tests but concentrations of CO and H_2 were too low as compared to that from predicted equilibrium model FLAME showing that gasification reaction did not reach equilibrium. This was demonstrated by the presence of high hydrocarbons in the products of the gasification zone.

The HRR in the gasification zone was 10 - 20% of the total HRR based on MLR in tests with airflow 9, 9.8, 12.8 g/(m^2.s) at heat flux 70 kW/m^2 and 14 g/(m^2.s) at heat flux 50 kW/m^2, showing that the box enclosure of cone calorimeter acted successfully as a gasifier.

6 REFERENCES

[1] A. Demirbaş, Biomass resource facilities and biomass conversion processing for fuels and chemicals. Energy Conversion and Management, (2001), **42**(11): pag. 1357-1378.

[2] F.R. Spellman, Forest-based biomass energy: concepts and applications, Energy and the Environment, ed. A. Ghassemi, Taylor & Francis Group, CRC Press, New York, (2012), pag. 281.

[3] Centre-for-sustainable-energy, (2007), A guide to small-scale wood fuel (biomass) heating systems, [Online]. Forestry Commisson England. Available: http://www.cse.org.uk/pdf/sof1113.pdf [Accessed 6th June 2014].

[4] Y. Cao, Y. Wang, J.T. Riley, and W.-P. Pan, A novel biomass air gasification process for producing tar-free higher heating value fuel gas. Fuel Processing Technology, (2006), **87**(4): pag. 343-353.

[5] A.L. Galindo, E.S. Lora, R.V. Andrade, S.Y. Giraldo, R.L. Jaén, and V.M. Cobas, Biomass gasification in a downdraft gasifier with a two-stage air supply: Effect of operating conditions on gas quality. Biomass and Bioenergy, (2014), **61**(0): pag. 236-244.

[6] M. Werrel, J.H. Deubel, S. Krüger, A. Hofmann, and U. Krause, The calculation of the heat release rate by oxygen consumption in a controlled-atmosphere cone calorimeter. Fire and Materials, (2014), **38**(2): pag. 204-226.

[7] The-British-Standards-Institution, Guidelines for assessing the fire threat to people, BSI Standards Limited: Switzerland, (2011), BS ISO 19706:2011. pag. 4.

[8] W.M. Pitts, The global equivalence ratio concept and the formation mechanisms of carbon monoxide in enclosure fires. Progress in Energy and Combustion Science, (1995), **21**(3): pag. 197-237.

[9] C. Huggett, Estimation of rate of heat release by means of oxygen consumption measurements. Fire and Materials, (1980), **4**(2): pag. 61-65.

[10] V. Babrauskas, Hazard Calculations, in SFPE Handbook of Fire Protection Engineering. 3rd ed. National Fire Protection Association: Quincy, Massachusetts, (2002), pag. 3-49.

[11] B. Daham, G.E. Andrews, H. Li, R. Ballesteros, M.C. Bell, J. Tate, and K. Ropkins, Application of a portable FTIR for measuring on-road emissions. SAE Technical paper series, (2005), DOI: 10.4271/2005-01-0676.

[12] P. Quaak, H. knoef, and H. Stassen, Energy from biomass: A review of combustion and gasification technologies, Energy Series, World Bank Technical Paper No. 422, The World Bank, Washington D.C., (1999), pag. 8.

[13] S.H. Chan., An exhaust emissions based air-fuel ratio calculation for internal combustion engines. Proc. Instn Mech Engrs, Part D: Journal of automobile engineering, (1996), **210**: pag. 273-280.